

Long-range order in quadrupolar systems on spherical surfaces – SUPPLEMENTARY INFORMATION

Andraž Gnidovec and Simon Čopar

University of Ljubljana, Faculty of Mathematics and Physics, SI-1000 Ljubljana, Slovenia

1 Additional results

In the main article, we showed several examples of ordering in quadrupolar systems on different Thomson lattices. We argue that the local arrangement of quadrupoles as well as global positional symmetry both contribute to the resulting quadrupolar order. As the Thomson lattice represents only one way of uniformly distributing points on a sphere, we further look to confirm this by exploring the quadrupolar states on the Tammes and Fibonacci lattices. The Tammes lattice is locally triangular and thus structurally similar to the Thomson lattice, whereas the Fibonacci lattice¹ becomes locally square around the equator as we increase the system size.

A comparison of configurations at $N = 72$ for different lattices is presented in Fig. 1. The ground state on the icosahedral Thomson lattice shows C_5 symmetry. Conversely, the Tammes lattice, while similar, lacks the high positional symmetry of the Thomson case, resulting in a ground state without any symmetries. The configuration shown in Fig. 1 is the only symmetric excited state and belongs to C_3 point group. Comparing Thomson and Tammes configurations, we observe in both cases the

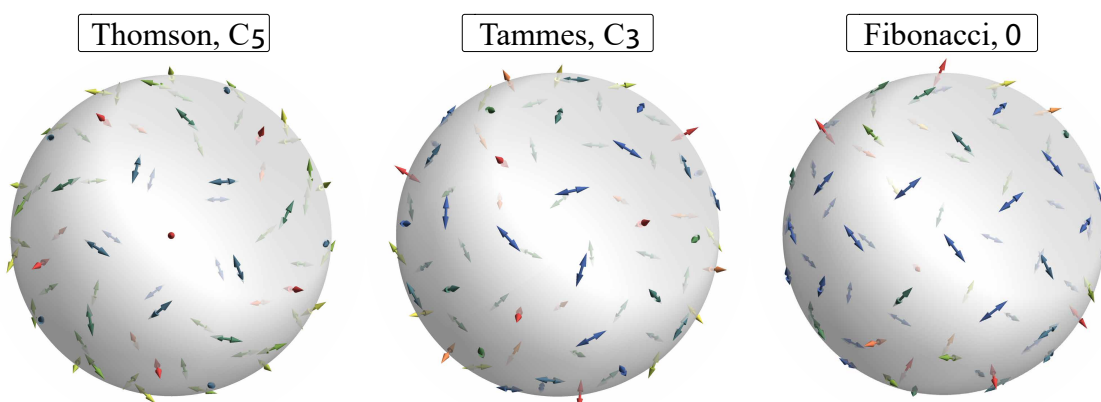


Figure 1: Comparison of configurations on different spherical lattices at system size $N = 72$.

tendency of quadrupoles to form pinwheel structures, at least in the vicinity of the symmetry axis. The situation differs substantially when we look at the configuration on the Fibonacci lattice. Locally square distribution of points around the equator results in the formation of windmill structures, similar

¹We parametrize the Fibonacci lattice of size N in spherical coordinates as

$$(\theta_k, \phi_k) = \left(\arccos \left[\frac{2k}{N+1} - 1 \right], 2\pi(2-\alpha)k \right),$$

where $\alpha = \frac{\sqrt{5}-1}{2}$ is the golden ratio and $k = 1 \dots N$. Different definitions are possible but they result in a structurally similar lattice.

to what we observe on planar square lattice. Around the poles, the lattice is highly irregular and long-range order is absent.

The choice of using a deterministic minimization method for investigating quadrupolar systems on a sphere limits the maximal system size we are able to explore to $N \approx 150$. Nevertheless, we argue that this is enough to discern ordering trends in bigger systems. Figure 2 shows ground state configurations for $N = 150$ tetrahedral Thomson lattice and $N = 100$ Fibonacci lattice. The former shows emergent pinwheel structures over the whole surface of the sphere, however, the arrangement of lattice defects does not support higher symmetry ordering (as e.g. in the case for $N = 122$) and the configuration only shows C_2 symmetry. Nevertheless, the configuration supports our assumption that in the limit of high N , quadrupolar systems on locally triangular lattices transition towards a pinwheel ground state (away from lattice defects) as the role of curvature decreases. This is further corroborated by lower values of out-of-plane parameter ξ for all configurations found at this system size ($0.30 \lesssim \xi \lesssim 0.38$, ground state value $\xi_{GS} = 0.303$) compared to values of ξ at smaller N . The Fibonacci configuration at $N = 100$ shows similar behavior to the $N = 72$ case in Fig. 1 but with a much wider windmill region. This results in the out-of-plane parameter value of $\xi = 0.198$ which is smaller than the pinwheel-limited value of $1/4$ for locally triangular lattices (in the limit of high system sizes).

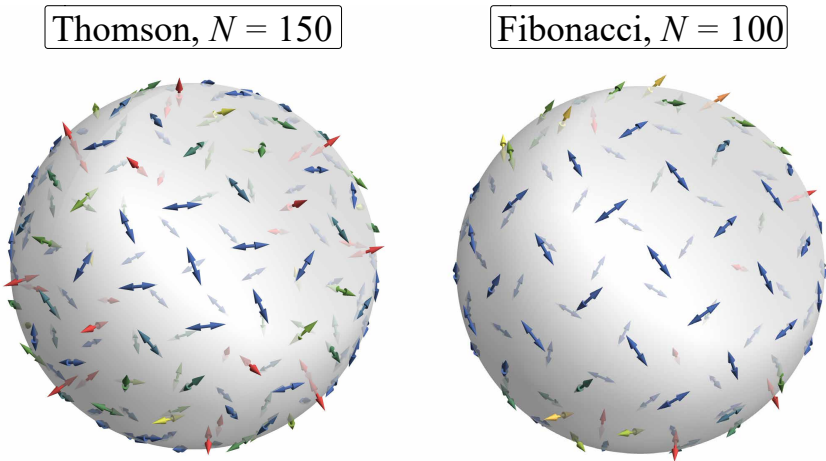


Figure 2: Examples of Thomson and Fibonacci quadrupolar ground states at higher system sizes.

2 Tables of optima

Below, we list lowest energy configuration results, along with configurations with the highest symmetry at given N , for systems of linear quadrupoles both the Thomson and Tammes lattices. The energy values correspond to the quadrupole tensor eigenvalues that satisfy $\text{Tr}(Q^2) = 1$.

N	E_{GS}	PG_{GS}	E_{sym}	PG_{sym}
10	-17.94614	0	-14.79685	C_2
11	-25.87675	0	-24.98204	C_2
12	-30.76187	S_6	-30.76187	S_6
13	-44.19957	0	-44.19957	0
14	-55.17387	0	-47.42441	C_6
15	-71.38314	0	-69.48079	C_3
16	-85.16844	0	-81.26653	T
17	-115.1684	C_2	-115.1684	C_2
18	-132.0108	C_2	-132.0108	C_2
19	-165.4244	0	-164.6409	C_2
20	-190.3918	0	-181.4474	C_2
21	-231.9683	C_2	-231.9683	C_2
22	-266.2751	S_4	-266.2751	S_4
23	-311.1626	0	-304.6335	C_2
24	-350.321	C_3	-350.0883	C_4
25	-425.6512	0	-425.6512	0
26	-475.3702	0	-447.0872	C_2
27	-553.6096	C_5	-553.6096	C_5
28	-595.3587	0	-580.0058	C_2
29	-696.4318	0	-689.0495	C_2
30	-780.5806	0	-772.0964	C_2
31	-852.7957	0	-842.0158	C_3
32	-944.3894	S_{10}	-944.3894	S_{10}
33	-1095.938	0	-1095.938	0
34	-1227.507	C_2	-1205.856	D_2
35	-1387.788	0	-1387.788	0
36	-1507.733	0	-1427.541	C_2
37	-1629.9	C_5	-1629.9	C_5
38	-1899.729	S_{12}	-1899.729	S_{12}
39	-1923.571	C_2	-1896.799	C_3
40	-2077.554	0	-2024.524	C_3
41	-2266.805	C_2	-2266.805	C_2
42	-2483.26	0	-2420.833	C_2
43	-2685.682	0	-2685.682	0
44	-3153.106	O	-3153.106	O
45	-3203.02	0	-3192.192	C_2
46	-3433.877	C_2	-3296.245	D_2
47	-3780.18	0	-3780.18	0
48	-4099.089	C_4	-4056.577	D_4
49	-4377.138	0	-4232.584	C_3
50	-4722.145	S_{10}	-4722.145	S_{10}
51	-5071.913	0	-5071.913	0
52	-5311.184	C_3	-5311.184	C_3
53	-5771.033	0	-5641.892	C_2
54	-6121.877	0	-6001.246	C_2
55	-6527.448	0	-6490.042	C_2
56	-6869.911	0	-6740.875	C_2
57	-7390.209	C_3	-7390.209	C_3

N	E_{GS}	PG_{GS}	E_{sym}	PG_{sym}
58	-7847.213	C_2	-7847.213	C_2
59	-8421.899	0	-8292.696	C_2
60	-8729.22	0	-8707.275	C_3
61	-9427.155	0	-9427.155	0
62	-9841.105	0	-9675.032	C_5
63	-10541.75	0	-10497.81	C_2
64	-11218.07	0	-10629.97	C_2
65	-11800.14	0	-11696.37	C_2
66	-12593.85	0	-12593.85	0
67	-12792.58	0	-12666.86	C_2
68	-13687.36	0	-13250.64	C_2
69	-14379.16	C_3	-14379.16	C_3
70	-15305.46	S_4	-15305.46	S_4
71	-15937.29	0	-15937.29	0
72	-16265.76	C_5	-16265.76	C_5
73	-17581.62	0	-17217.24	C_2
74	-18796.39	0	-18796.39	0
75	-19333.59	0	-19188.43	C_3
76	-20496.73	0	-20496.73	0
77	-20785.71	C_5	-20785.71	C_5
78	-21890.22	C_2	-21675.97	S_6
79	-22887.72	0	-22887.72	0
80	-24140.24	0	-23691.7	C_4
81	-25375.87	0	-25166.6	C_2
82	-26399.32	0	-26314.82	C_2
83	-27664.05	0	-27376.7	C_2
84	-29065.02	0	-28927.9	C_2
85	-29901.36	0	-29554.66	C_2
86	-31580.65	0	-31580.65	0
87	-32441.53	0	-32272.87	C_2
88	-33681.07	0	-33681.07	0
89	-35199.35	0	-35006.52	C_2
90	-36214.78	0	-36214.78	0
91	-37825.44	0	-37636.89	C_2
92	-39411.5	0	-39411.5	0
93	-41005.54	0	-41005.54	0
94	-42724.3	C_2	-42724.3	C_2
95	-44286.94	0	-43545.95	C_2
96	-46302.03	0	-46302.03	0
97	-47523.83	0	-47523.83	0
98	-49221.05	0	-49221.05	0
99	-51178.49	0	-50711.02	C_2
100	-52712.89	0	-52638.11	C_3
122	-105055.6	I	-105055.6	I
132	-139470.9	C_5	-139470.9	C_5
136	-155127.9	0	-155127.9	0
150	-228044.5	C_2	-220168.9	D_2

Table 1: Ground state and highest symmetry solutions on the Thomson lattices.

N	E_{GS}	PG_{GS}	E_{sym}	PG_{sym}
10	-17.85698	0	-17.25249	C_2
11	-26.26433	0	-26.26433	0
12	-30.76187	S_6	-30.76187	S_6
13	-45.38164	0	-44.61766	C_4
14	-59.1275	C_2	-58.55624	S_4
15	-74.68377	0	-74.68377	0
16	-96.20829	S_8	-96.20829	S_8
17	-114.0142	C_2	-114.0142	C_2
18	-131.9526	0	-131.9526	0
19	-168.5474	0	-168.5474	0
20	-188.9719	0	-180.5959	C_2
21	-229.2873	0	-229.2873	0
22	-275.1527	0	-275.1527	0
23	-325.674	0	-325.674	0
24	-351.5055	C_4	-351.5055	C_4
25	-440.1661	0	-433.6832	C_3
26	-512.0153	0	-512.0153	0
27	-549.2657	0	-549.2657	0
28	-656.3142	0	-656.3142	0
29	-731.1445	0	-731.1445	0
30	-783.7615	0	-780.4043	D_3
31	-898.9203	C_5	-898.9203	C_5
32	-957.8877	0	-921.6676	C_3
33	-1140.2	0	-1088.901	C_3
34	-1275.227	0	-1275.227	0
35	-1386.337	0	-1386.337	0
36	-1546.171	0	-1546.171	0
37	-1733.916	0	-1733.916	0
38	-1909.507	S_{12}	-1909.507	S_{12}
39	-2033.533	0	-2033.533	0
40	-2240.636	C_3	-2240.636	C_3
41	-2488.956	0	-2488.956	0

N	E_{GS}	PG_{GS}	E_{sym}	PG_{sym}
42	-2586.568	0	-2547.455	C_2
43	-2857.83	0	-2857.83	0
44	-3073.318	C_2	-3073.318	C_2
45	-3331.461	0	-3331.461	0
46	-3665.802	0	-3665.802	0
47	-3903.933	0	-3903.933	0
48	-4180.57	C_4	-4107.373	D_4
49	-4631.788	0	-4512.917	C_2
50	-4746.23	C_2	-4736.893	C_6
51	-5284.134	0	-5284.134	0
52	-5684.646	0	-5653.811	C_3
53	-6128.256	0	-6128.256	0
54	-6538.604	C_2	-6538.604	S_4
55	-6800.163	0	-6800.163	0
56	-7245.993	0	-7187.049	C_2
57	-7657.339	0	-7657.339	0
58	-8128.102	0	-7848.924	C_2
59	-8694.171	0	-8694.171	0
60	-9022.76	0	-9022.76	0
61	-9632.079	0	-9603.014	C_2
62	-10267.12	C_2	-10267.12	C_2
63	-10652.79	0	-10597.55	C_2
64	-11566.38	0	-11566.38	0
65	-12224.11	0	-12042.76	C_2
66	-12494.04	0	-12373.88	C_3
67	-13538.89	0	-12915.27	C_2
68	-14224.9	0	-14224.9	0
69	-14688.46	0	-14688.46	0
70	-15824.37	0	-15824.37	0
71	-16407.1	0	-16407.1	0
72	-16933.5	0	-16785.31	C_3

Table 2: Ground state and highest symmetry solutions on the Tammes lattices.